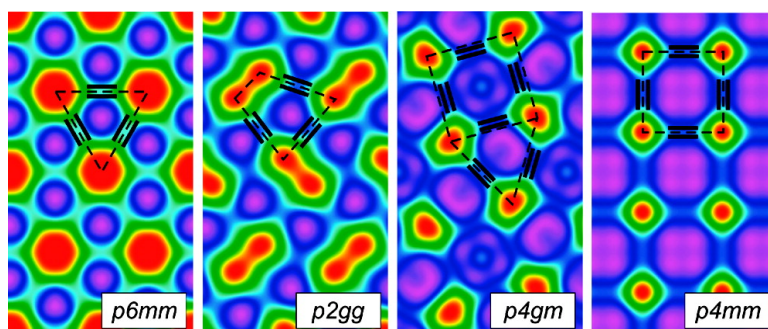


The Trapezoidal Cylinder Phase: A New Mode of Self-Assembly in Liquid-Crystalline Soft Matter

Feng Liu, Bin Chen, Benjamin Glettner, Marko Prehm, Malay Kumar Das, Ute Baumeister, Xiangbing Zeng, Goran Ungar, and Carsten Tschierske

J. Am. Chem. Soc., **2008**, 130 (30), 9666-9667 • DOI: 10.1021/ja8038932 • Publication Date (Web): 03 July 2008

Downloaded from <http://pubs.acs.org> on February 8, 2009



More About This Article

Additional resources and features associated with this article are available within the HTML version:

- Supporting Information
- Access to high resolution figures
- Links to articles and content related to this article
- Copyright permission to reproduce figures and/or text from this article

[View the Full Text HTML](#)

The Trapezoidal Cylinder Phase: A New Mode of Self-Assembly in Liquid-Crystalline Soft Matter

Feng Liu,[†] Bin Chen,[‡] Benjamin Glettner,[‡] Marko Prehm,^{‡,§} Malay Kumar Das,[§] Ute Baumeister,[§] Xiangbing Zeng,[†] Goran Ungar,^{*,†} and Carsten Tschierske^{*,‡}

Department of Engineering Materials, University of Sheffield, Mappin Street, Sheffield S1 3JD, Great Britain, Organic Chemistry, Institute of Chemistry, Martin-Luther-University Halle-Wittenberg, Kurt-Mothes Str. 2, D-06120 Halle, Germany, and Physical Chemistry, Institute of Chemistry, Martin-Luther-University Halle-Wittenberg, Mühlporfte 1, D-06108 Halle, Germany

Received May 23, 2008; E-mail: g.ungar@sheffield.ac.uk; carsten.tschierske@chemie.uni-halle.de

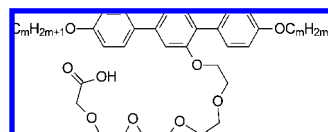
Organization of functional molecules in defined two-dimensional (2D) arrays is of current interest owing to potential nanotechnological applications. The design of polygonal nets using coordination polymers¹ and by structural DNA nanotechnology has received considerable attention,² but most 2D arrays were obtained on solid surfaces.³ Recently, in the field of soft matter engineering, a series of new types of liquid-crystalline (LC) phases, representing polygonal cylinder arrays ranging from trianglular^{4d} via square, pentagonal, hexagonal to giant cylinder structures, were obtained by self-assembly of T-shaped ternary block molecules.^{4,5} In all these polygonal 2D nets and cylinder arrays, the sides were formed by identical building blocks.

Here we report the first polygonal net where one of the sides has a different length and is composed of a different material than the others. This leads to a new LC phase representing an array of cylinders with trapezoidal cross section. More generally, the possibility of having different types of cylinder walls in a uniform periodic structure provides a new tool for enhancing complexity of self-assembled systems. This tiling pattern was obtained with T-shaped facial amphiphilic triblock molecules **1** and **2** in which a rigid rod-like *p*-terphenyl unit is substituted laterally with a polar and flexible oligoethylene glycol chain terminated by a hydrogen-bonding COOH group (**1**) or by a Li carboxylate group (**2**) and having either identical (**1**) or different (**2**) alkyl chains in the terminal positions (for synthesis, see the Supporting Information). Nanoscale segregation of the three distinct segments,^{5a} combined with attractive intermolecular hydrogen bonding^{4a,b,d,5} or ionic interaction,^{4c} respectively, plays a key role in self-assembly of these compounds.

Phase assignment is based on polarizing microscopy and X-ray diffraction, including electron density reconstruction. Between crossed polarizers, all compounds **1a–d** (Table 1) and **2a–d** (Table 2) show optical textures typical of LC phases with 2D periodicity (columnar phases, see Figures 1c, and S2–S9). The X-ray diffraction patterns show diffuse wide angle scatterings with a maximum around 0.45 nm, confirming the LC nature of all mesophases (Figures S4–S6). Indexing of the SAXS patterns leads to the phase assignments with plane groups shown in Tables 1 and 2 (see also Figures S2–S9, Tables S3–S8).

Attention is first drawn to compound **1c**, which shows two LC phases between 45 and 52 °C with a first-order phase transition at *T* = 49 °C (Figure S1a). Above 49 °C, the diffraction pattern is

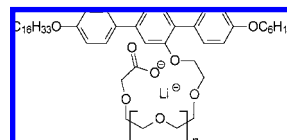
Table 1. Data on Acids **1a–f**^a



No.	<i>m</i>		<i>T</i> /°C		<i>a</i> , <i>b</i> /nm
1a ^{4a}	8	Cr 21 Col _{squ} /p4gm	30	Col _{squ} /p4mm 31 Iso	7.7, 2.5 ^b
1b	9	Cr 19 Col _{squ} /p4gm	41	Iso	8.1
1c	10	Cr 45 Col _{rec} /p2gg	49	Col _{hex} Δ/p6mm 52 Iso	8.4, 4.7, 4.6 ^c
1d	11	Cr 52 Col _{rec} /p2gg	55	Iso	8.5, 5.0
1e ^{4c}	12	Cr 59 (Col _{rec} /p2gg 54)	SmA 67	Iso	8.9, 5.0
1f	16	Cr 74 SmA	92	Iso	

^a Abbreviations: Cr = crystalline solid, Iso = isotropic liquid, SmA = smectic A phase; Col_{squ}/p4gm = square columnar phase with plane group *p4gm* (square and triangular cylinders, 1:1 ratio), Col_{squ}/p4mm = square columnar phase with plane group *p4mm* (square cylinders), Col_{rec}/p2gg = rectangular columnar phase with plane group *p2gg* (trapezoidal cylinders, highlighted), Col_{hex}Δ/p6mm hexagonal columnar phase with plane group *p6mm* (triangular cylinders); the structures of the cylinder LC phases are shown in Figure 2a–d. ^b Col_{squ}/p4mm phase. ^c Col_{hex}Δ/p6mm phase.

Table 2. Data on Li Salts **2a–d**^a



No.	<i>n</i>		<i>T</i> /°C		<i>a</i> , <i>b</i> /nm	<i>n</i> _{cell}	<i>n</i> _{wall}
2a	1	Cr 74 Col _{hex} Δ/p6mm	93	Iso	5.0	8.0	2.7
2b	2	Cr 56 Col _{rec} /p2gg	81	Iso	9.5, 5.3	16.9	2.8
2c	3	Cr 56 Col _{squ} /p4gm	83	Iso	9.2	27.2	2.7
2d	4	Cr 53 Col _{squ} /p4mm	87	Iso	4.3	5.8	2.9

^a *n*_{cell} = number of molecules per unit cell with an assumed height of 0.45 nm, *n*_{wall} = number of molecules in the cross section of the cylinder walls; for details, see Table S8; for the abbreviations, see Table 1.

characterized by one strong and two weak reflections indexed as (10), (11), and (20) of a hexagonal lattice with the cell parameter *a*_{hex} = 4.6 nm (Figure S3d,e). This is a triangular cylinder phase, which was recently analyzed in detail for a similar compound.^{4d} However, our main focus here is on the low-temperature phase. The SAXS reflections of this mesophase (Figure 1a) can be indexed on a rectangular lattice with parameters *a* = 8.4 nm and *b* = 4.7 nm, plane group *p2gg*. This is confirmed by the 2D pattern from an aligned sample shown in Figure 1b (see also Figure S3). The electron density map reconstructed from the small angle diffraction

[†] University of Sheffield.
[‡] Organic Chemistry, Institute of Chemistry, Martin-Luther-University Halle-Wittenberg.
[§] Physical Chemistry, Institute of Chemistry, Martin-Luther-University Halle-Wittenberg.

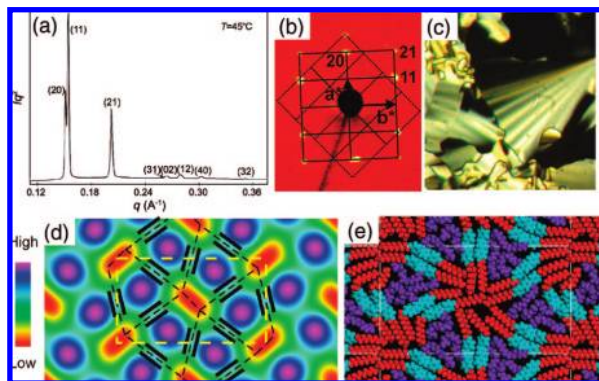


Figure 1. Trapezoidal cylinder phase: (a) SAXS powder pattern of **1c** at 45 °C; (b) SAXS of an aligned sample of **1c** at 46 °C with reciprocal lattices for two domains and indices for the observed reflections; (c) texture as seen for **1d** between crossed polarizers ($T = 50$ °C); (d) electron density map as reconstructed from the diffraction pattern in (a); (e) snapshot of a molecular dynamics simulation of **1c**; for easy comparison with (d), color coding is as follows: red = alkyl chains (lowest electron density), light blue = terphenyl groups (intermediate), purple = oligo(oxyethylene) groups (highest density); (d,e) are viewed along the column long axis.

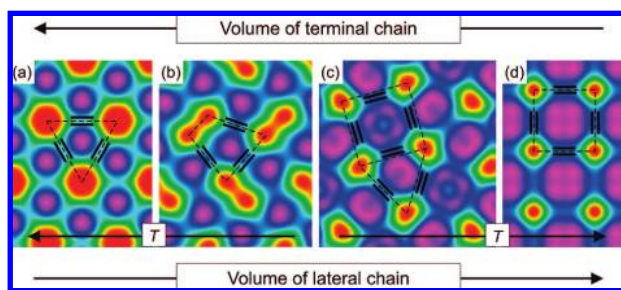


Figure 2. Electron density maps of compounds **2a–d**: (a) **2a**, $Col_{hex}\Delta/p6mm$; (b) **2b**, $Col_{rec}/p2gg$; (c) **2c**, $Col_{squ}/p4gm$; (d) **2d**, $Col_{squ}/p4mm$; arrows indicate the effects of the volume of lateral and terminal chains, as well as temperature: color code as in Figure 1d.

intensities of the powder pattern (synchrotron radiation, see Figure 1d) shows six high electron density regions (blue/purple) grouped around each low electron density region (yellow/red). The high electron density regions contain the polyether chains and carboxyl groups, while the aliphatic chains form the low electron density regions which have an elliptical cross section. Considering the molecular topology with alkyl chains at the ends and a polyether chain at a side of a rigid aromatic core, it is concluded that the rod-like units (dark lines in Figure 1d) separate the high electron density regions and form three walls of a cylinder. The fourth wall, somewhat shorter than the other three, is the elliptical aliphatic column, or ribbon (red/yellow). The edges of these ribbons also act as junctions connecting the aromatic walls at the corners opposite the aliphatic wall. This leads to an array of cylinders with an overall trapezoidal shape. In a hypothetical 3D unit cell with the experimental 2D unit cell base and a height equal to an assumed one-molecule thickness of 0.45 nm (maximum of the diffuse wide angle scattering), the number of molecules is calculated as $n_{cell} = 13.7$ on average (see Table S9). Since there are 6 aromatic walls per unit cell, this means that the average thickness of the walls formed by the rod-like cores is 2.3 terphenyl units placed side-by-side. This is a typical value for polygonal cylinder phases of facial amphiphiles.^{4b} Figure 1e shows a snapshot of annealing molecular dynamics simulation of one molecular layer ($c = 0.45$ nm) with periodic boundaries defined laterally by the experimentally determined unit cell. The simulation confirms efficient space filling and phase separation achieved in the proposed structure.

The new structure can be regarded as a slightly distorted triangular cylinder phase where the circular alkyl columns are deformed elliptically. This deformation is attributed to the reduction in conformational disorder of the alkyl chains at reduced temperatures, as the more extended chains tend toward more parallel packing in ribbons. Such packing is favored at lower temperatures and for longer chains. In **1d**, a higher homologue of **1c** with longer alkyl chains (see Table 1), the triangular cylinder phase ($Col_{hex}\Delta/p6mm$) disappears completely, being replaced by the trapezoidal cylinder phase ($Col_{rec}/p2gg$). Further chain elongation, however, leads to fusion of aliphatic regions which gives rise to the formation of a layer structure (SmA phase of **1f**). In contrast, reduction of the alkyl chain length reduces the effective length of the molecule, that is, of the sides of the polygon. As a result, the number of sides of the polygon must increase. Indeed, compounds **1a** and **1b** with shorter alkyl groups display $Col_{squ}/p4gm$ (squares + triangles) and $Col_{squ}/p4mm$ (only squares) phases.

A phase sequence $Col_{hex}\Delta/p6mm$ (triangles), $Col_{rec}/p2gg$ (trapezes), $Col_{squ}/p4gm$ (squares+triangles), $Col_{squ}/p4mm$ (squares) was observed for the series of Li salts **2a–d** by increasing the length of the lateral chain at constant alkyl chain length (Table 2 and Figure 2). The fact that the trapezoidal cylinder phase is formed by different compounds indicates that this is a fundamentally new and general phase structure in T-shaped ternary amphiphiles. The mixed wall trapezoidal cylinders provide two advantages over the all-aromatic wall cylinders: (a) they allow improved packing of the relatively long and rigid alkyl chains, and (b) they provide more interior space than the related triangular cylinders.

In summary, a LC phase is reported in polyphilic molecules based on a new polygonal tiling pattern. In this trapezoidal phase, for the first time, not all walls of the polygonal nanocylinders are made of the same material. This provides a new variable for increasing the complexity in LC engineering and proves again the almost limitless potential of the general concept of polyphilic tectons in the design of new complex soft matter structures.

Acknowledgment. This work, as part of the ESF EUROCORES Programme SONS, was supported by funds from the DFG, EPSRC, and the EC 6th Framework Programme, under contract ERAS-CT-2003-989409. F.L. is grateful to the University of Sheffield for a scholarship. We thank Dr. P. Boesecke for help with the experiment on station ID02, and ESRF for the beamtime.

Supporting Information Available: Textures, analytical, calorimetric, and X-ray data and synthesis. This material is available free of charge via the Internet at <http://pubs.acs.org>.

References

- Moulton, B.; Zaworotko, M. J. *Chem. Rev.* **2001**, *101*, 1629–1658.
- (a) Furukawa, S.; Uji-i, H.; Tahara, K.; Ichikawa, T.; Sonoda, M.; De Schryver, C.; Tobe, Y.; De Feyter, S. *J. Am. Chem. Soc.* **2006**, *128*, 3502–3503. (b) Feldkamp, U.; Niemeyer, C. M. *Angew. Chem., Int. Ed.* **2006**, *45*, 1856–1876. (c) Lin, C.; Liu, Y.; Rinker, S.; Yan, H. *ChemPhysChem* **2006**, *7*, 1641.
- Zhou, H.; Dang, H.; Yi, J.-H.; Nanci, A.; Rochefort, A.; Wuest, J. D. *J. Am. Chem. Soc.* **2007**, *129*, 13774–13775. (a) Stepanow, S.; Lin, N.; Payer, D.; Schlickum, U.; Klappenberger, F.; Zoppellaro, G.; Ruben, M.; Brune, H.; Bart, J. V.; Kern, K. *Angew. Chem., Int. Ed.* **2007**, *46*, 710–713.
- (a) Chen, B.; Zeng, X. B.; Baumeister, U.; Ungar, G.; Tschierske, C. *Science* **2005**, *307*, 96–99. (b) Chen, B.; Baumeister, U.; Pelzl, G.; Das, M. K.; Zeng, X.-B.; Diele, S.; Ungar, G.; Tschierske, C. *J. Am. Chem. Soc.* **2005**, *127*, 16578–16591. (c) Cook, A. G.; Baumeister, U.; Tschierske, C. *J. Mater. Chem.* **2005**, *15*, 1708–1721. (d) Liu, F.; Chen, U. B.; Baumeister, U.; Zeng, X.; Ungar, G.; Tschierske, C. *J. Am. Chem. Soc.* **2007**, *129*, 9578–9579.
- (a) Tschierske, C. *Chem. Soc. Rev.* **2007**, *36*, 1930–1970. (b) Cheng, X. H.; Prehm, M.; Das, M. K.; Kain, J.; Baumeister, U.; Diele, S.; Leine, D.; Blume, A.; Tschierske, C. *J. Am. Chem. Soc.* **2003**, *125*, 10977–10996. (c) Prehm, M.; Liu, F.; Baumeister, U.; Zeng, X.; Ungar, G.; Tschierske, C. *Angew. Chem., Int. Ed.* **2007**, *46*, 7972–7975.

JA8038932